Direct capture in the 3^+ resonance of $^2H(\alpha,\gamma)^6Li$

P. Mohr, V. Kölle, S. Wilmes, U. Atzrott, and G. Staudt
Physikalisches Institut der Universität Tübingen, D-72076 Tübingen, Germany

J. W. Hammer
Institut für Strahlenphysik, Universität Stuttgart, D-70569 Stuttgart, Germany

H. Krauss and H. Oberhummer
Institut für Kernphysik, TU Wien, A-1040 Wien, Austria
(Received 5 May 1994)

The cross section for the capture reaction $^2H(\alpha,\gamma)^6Li$ was measured in the energy range of about $E_{\alpha,\text{lab}} \approx 2$ MeV corresponding to the 3^+ resonance in ^6Li at $E_x = 2186$ keV. Calculations in a direct-capture model using double-folded α-d potentials reproduce strength and width of this resonance as well as the nonresonant capture cross section at lower and higher energies.

PACS number(s): 24.10.Ht, 24.30.−v, 24.50.+g, 25.55.−e

I. INTRODUCTION

It is generally supposed that essentially all ^{6}Li observed in the universe is produced by spallation reactions via galactic cosmic rays. The only mechanism to produce significant amounts of ^{6}Li in the early universe is the radiative capture of the deuteron by an α particle [1,2]. Therefore there has been much interest in the study of the $^2H(\alpha,\gamma)^6Li$ at low energies recently.

The capture cross section has first been measured by Robertson *et al.* [3] for projectile energies 1 MeV $\leq E_{\text{c.m.}} \leq 3$ MeV by using a magnetic analysis technique to detect the recoiling ^{6}Li ions. Recently, the low-energy range ($E_{\text{c.m.}} \leq 500$ keV) has been analyzed using Coulomb dissociation of the ^{6}Li nucleus in the Coulomb field of a ^{208}Pb nucleus [4,5]. Hesselbarth *et al.* [4] have measured the breakup of 60 MeV ^{6}Li scattered from ^{208}Pb inside the grazing angle for c.m. energies of the fragments between 100 keV and 1.5 MeV whereas Kiener *et al.* [5] have studied the breakup of 156 MeV ^{6}Li projectiles at ^{208}Pb with small emission angles of the α particles and deuteron fragments. Shyam *et al.* [6] studied theoretically the interplay of nuclear and Coulomb contributions to breakup processes, which is relevant for the extraction of the astrophysical S factor for the reaction $^2H(\alpha,\gamma)^6Li$. Their calculations suggest that higher beam energies provide a more favorable regime for the extraction of S factors of the radiative capture processes from measurements of the breakup cross sections.

Theoretically, the capture cross section of $^2H(\alpha,\gamma)^6Li$ was calculated by Robertson *et al.* in terms of a direct-capture model (DC) [3]. Langanke has studied the reaction in the framework of a microscopic potential model assuming that the process is predominantly electric quadrupole radiation ($E2$) [7]. In a further calculation Langanke and Rolfs [8] took into account the internal quadrupole moment of the deuteron and a small D-state component in the ^{6}Li ground state. D-state and tensor interaction effects have been studied by Crespo *et al.* [9,10] in a deuteron-α-particle DC model. Burkova *et al.* [11], Typel *et al.* [12], and Jang [13] analyzed the small electric dipole contribution ($E1$) to the capture cross section. However, Typel *et al.* [12] found that $E1$ capture noticeably contributes to the $^2H(\alpha,\gamma)^6Li$ cross section at astrophysical energies. In magnitude their $E1$ cross section roughly agrees with the one already estimated by Robertson *et al.* [3] while it is clearly smaller than the value obtained by the calculation of Burkova *et al.* [11].

The contribution to the capture cross section of the two $T = 1$ resonances in ^{6}Li is very small. The $T = 0$ particles in the entrance channel cannot couple to any state with $T \neq 0$. Thus only the $T = 0$ admixture of the $T = 1$ resonances can influence the capture cross section which is estimated to be only about 1% [3].

In the energy range between 500 and 900 keV the capture cross section is strongly dominated by the 3^+ resonance at $E_{\text{c.m.}} = 711$ keV corresponding to the first exited state in ^{6}Li at $E_x = 2186$ keV.

The total width of this resonance is well known [14]. The radiative width was determined by Eigenbrod via inelastic electron scattering [15] and by Kiener *et al.* [16] via the sequential breakup mode $^6Li \rightarrow {}^6Li^*(3^+) \rightarrow \alpha + d$ of 156 MeV ^{6}Li projectiles on ^{208}Pb. The $^2H(\alpha,\gamma)^6Li$ capture cross section was so far not determined directly in the region of the 3^+ resonance. Thus we have measured the capture γ rays in this energy range. Furthermore, we have calculated the capture cross section in resonant and nonresonant energy regions using a DC model.

II. EXPERIMENTAL SETUP

A. Accelerator and gas target

The experiment has been performed at the Stuttgart DYNAMITRON laboratory using the windowless and recirculating gas target facility RHINOCEROS. The win-

 ©1994 The American Physical Society

dowless gas target has been used in the extended setup with a target cell especially designed for this experiment (see Fig. 1). The volume of the cell had an active diameter of 35 mm and a thickness of only 22 mm. The active volume was limited at the axis of the beam by two watercooled apertures of 5 mm diameter, the cell being thus operated in transmission. The effective length of the gas chamber is given by the 70 mm distance between entrance and exit apertures. The deuterium target gas had a purity of 99.999%. The $^4He^+$ beam was stopped in a Faraday cup which was located about 150 cm behind the target cell to reduce the background by a large distance from the detectors. To minimize reactions of projectiles and recoils of the deuterium with the walls of the cell and the apertures, all these parts have been gold plated with a layer of 99.99% pure gold of 10–20 μm thickness. By this, background reactions could be reduced by a large amount, because one had to consider that the recoiled deuterium nuclei had up to 2/3 of the α energy which is high enough to produce background.

At last, inverse kinematics has been chosen for this experiment to reduce the neutron induced background which is expected to be stronger when a deuteron beam is used.

The pressure of the gas cell was reduced by four differential pumping stages (p_2-p_5, p_1 and p_2 being at the same pressure, see Fig. 1) of the gas target facility RHINOCEROS to a pressure of about 10^{-8} mbar in the beamline, the whole setup being reduced to the requirements of a rather low target pressure of 10 mbar. The gas was recirculated and purified in the mainstream by using a cryogenic zeolith trap and a special cryotrap. By this the gas impurities could be kept low for beam periods of several days. The gas pressure was monitored by an absolute measuring capacitance manometer with an accuracy of 2%. The cell pressure has been kept constant within 5% by manual regulation.

In order to measure the capture cross section of the reaction ^{2}H(α,γ)^{6}Li in the energy region of the 3^+ resonance (E_x=2186 keV), the α-beam energy was varied between $E_\alpha^{\rm lab}$ = 2.0 and 2.2 MeV. The beam-defining apertures were located about 500 mm in front of the target cell to keep a disturbing γ background low. The beam currents used were in the order of magnitude of 100 μA with a beam-energy resolution of 2 keV, and care was taken to produce a narrow beam profile of less than 2 mm

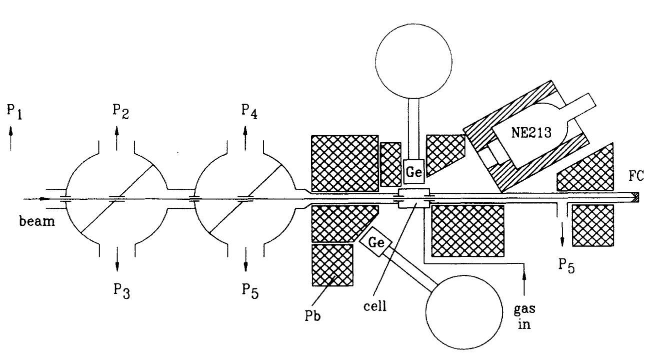

FIG. 1. Scheme of the experimental setup.

diameter. Because of secondary charge effects in the gas, the beam could only be monitored by the measurement of elastically scattered particles. For this purpose two silicon surface-barrier detectors for particles were set at an angle of 28° and 60°. Two apertures were placed in front of both detectors: a slit aperture (0.3 mm × 5.0 mm, distance from the beam axis d_1 = 18 mm) was used to define the effective target length for the particle detectors, and a circular aperture (radius r = 0.5 mm, distance to the beam axis d_2 = 234 mm) was used to define the solid angle: $\Delta\Omega = 1.43 \times 10^{-5}$ sr. The effective target length for the particle detectors was located in the center of the scattering chamber.

As already mentioned, the deuteron gas pressure in the cell was about 10 mbar. Corresponding to an effective gas target thickness of d = 70 mm the energy loss of the α particles in the target gas has been calculated to be $\Delta E_\alpha^{\rm lab}$ = 28 keV [17]. The total width of the 3^+ resonance in ^{6}Li is $\Gamma_{\rm c.m.} = 24 \pm 2$ keV [14]. Therefore in the laboratory system we obtain a width of $\Gamma_{\rm lab} = 3 * \Gamma_{\rm c.m.}$. Thus our experiment was performed in a thin-target geometry.

B. Experimental procedure

The emitted γ quanta were detected using a high-purity germanium detector [HPGe, 85% relative effiency compared to a 3 × 3 inch NaI(Tl) crystal]. Because of the finite dimensions of the HPGe detector (diameter ϕ = 7 cm) and the thickness of the reaction zone d the resulting γ peak is Doppler broadened. If one places the HPGe detector in close geometry at 90° relative to the beam axis and symmetrically to the center of the gas cell, one expects a Doppler width of the resulting γ peak of about $\Delta E_\gamma^{\rm broad.} \approx 60$ keV (see Fig. 2, upper part). If one places the HPGe detector again looking towards the center of the gas cell but at 130° relative to the beam axis, the Doppler width of the resulting peak is reduced to about $\Delta E_\gamma^{\rm broad.} \approx 20$ keV. Furthermore, the γ peak is Doppler shifted to lower energies: $\Delta E_\gamma^{\rm shift.} \approx 25$ keV (see Fig. 2, lower part). This Doppler shift was desired for a better separation of the γ peak to be expected from the background peak at 2222 keV which stems from the neutron capture reaction ^{1}H(n,γ)^{2}H. Some efforts have been done to minimize this background peak: The neutron production by (α,n) reactions along the beamline was reduced by precise beam alignment which could be controlled as well optically by emitted light in the gas cell as by the use of a neutron monitor (4 × 2 inch NE 213 with an efficient n-γ-discrimination). A second HPGe detector (HPGe, 30% relative effiency) was used as monitor during the whole experiment. The deadtime was determined to be smaller than 0.1 % in all γ and particle spectra by the use of test pulses. Therefore a deadtime correction was not necessary in this experiment.

With this setup about 100 γ spectra were recorded at the incident energy range of $E_\alpha^{\rm lab}$ between 2.0 and 2.2 MeV. Several examples are shown in Fig. 3. The γ counts were normalized to elastically scattered recoil deuterons and α particles from $^2H(\alpha,\alpha)^2H$. These particles were detected by use of a (light-tight) silicon detector which was mounted at a fixed position of 28° to the direction of the α beam and aligned to the center of the gas cell. A second particle detector at an angle of 60° was used as monitor. From the analysis of the particle spectra at 28° three results can be obtained.

(i) Because of the inverse kinematics used in our experiment, in the particle spectrum at $\vartheta_{lab} = 28°$ two α-particle peaks and one deuteron recoil peak are observed (see Fig. 4). The α energies sensitively depend on the scattering angle. Therefore this angle is very precisely determined.

(ii) The elastic cross section in the 3^+ resonance has already been measured by Galonsky *et al.* [18] and Meiner *et al.* [19]. Thus, in our experiment the beam energy in the center of the gas cell could be determined by the measured ratio $\sigma_d(\vartheta_{lab} = 28°)/\sigma_\alpha(\vartheta_{lab} = 28°)$ that corresponds to $\sigma(\vartheta_{c.m.} = 124°)/\sigma(\vartheta_{c.m.} = 96.9°)$. This ratio does not depend on the solid angle and the effective target length because it was measured using only one particle detector. In Fig. 5 this experimental ratio is compared to our folding model calculation (see Sec. III).

(iii) To obtain the total capture cross section for

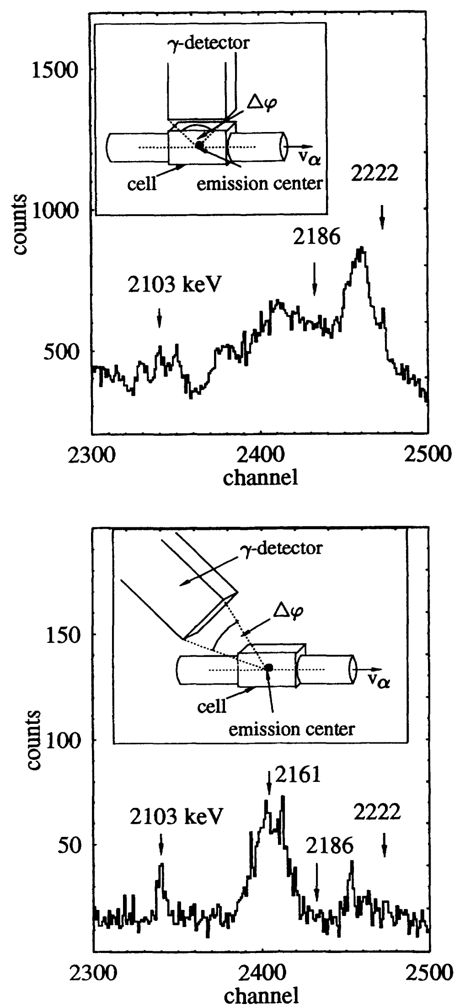

FIG. 2. γ spectra in the 3^+ resonance of $^2H(\alpha,\gamma)^6Li$, measured with a 85% HPGe detector placed at $\vartheta = 90°$ (upper part) and $\vartheta = 130°$ (lower part). The γ peak at 2186 keV is about 60 keV Doppler broadened (upper part), respectively, about 20 keV Doppler broadened and 25 keV shifted to lower energies (lower part).

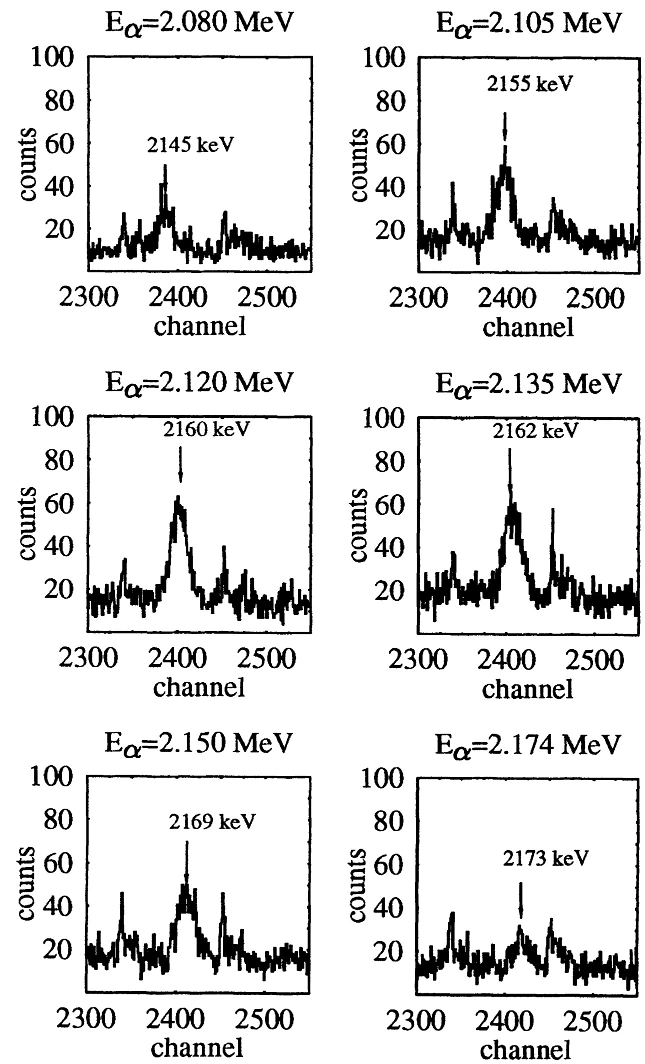

FIG. 3. γ spectra of $^2H(\alpha,\gamma)^6Li$ in the vicinity of the 3^+ resonance measured at $\vartheta = 130°$.

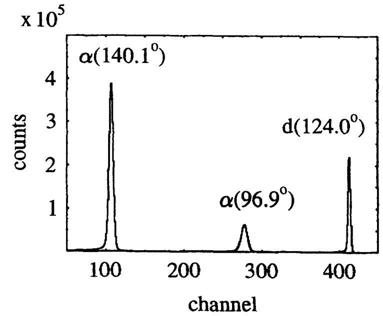

FIG. 4. Spectrum of the particle detector mounted at $\vartheta_{lab}=28°$. The angles in brackets are the center-of-mass scattering angles.

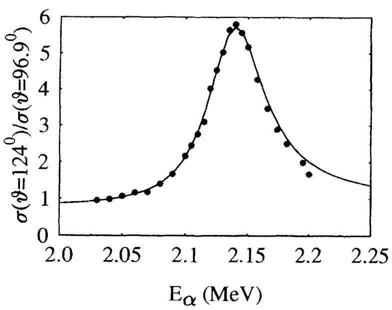

FIG. 5. Ratio of $\sigma(\vartheta_{\vartheta_{c.m.}} = 124°)/\sigma(\vartheta_{c.m.} = 96.9°)$ which can be measured using one particle detector at $\vartheta_{lab} = 28°$. The solid line is the result of the present OM calculation.

$^2H(\alpha,\gamma)^6Li$ the γ-ray intensity was normalized under consideration of the angular distribution of this $E2$ transition to the elastic scattering cross section at $\vartheta_{c.m.} = 96.9^o$ and the efficiency of the 85% HPGe detector which is determined by the following procedure.

A pointlike γ calibration source ^{226}Ra was moved along the beam axis through the gas cell. We measured the counting rate for the two γ energies $E_\gamma = 2204$ keV and 2448 keV. Then the total efficiency is given by the ratio of the number of detected to the number of emitted γ quanta: $\epsilon_{tot} = N_{det.}/N_{em.}$. The energy dependence of the total efficiency was smaller than about 5% for the two different γ energies measured at all positions of the γ source. Therefore we used the value obtained for $E_\gamma =$ 2204 keV and for positions of the source in the interior of the gas cell also for the γ quanta of $^2H(\alpha,\gamma)^6Li$ which were in an energy range of 2100 keV $\le E_\gamma \le$ 2200 keV: $\epsilon_{tot} = N_{det.}/N_{em.} = (1.42 \pm 0.05) \times 10^{-3}$ (see Fig. 6). The detection efficiency for the γ quanta which do not come from the interior of the gas cell can be neglected in our experiment because the pressure of the gas drops by more than one order of magnitude from the interior of the gas cell to the outside region.

III. D-α ELASTIC SCATTERING AND CLUSTER POTENTIALS

Phase shifts for d-α elastic scattering were extracted from excitation functions of differential cross sections and

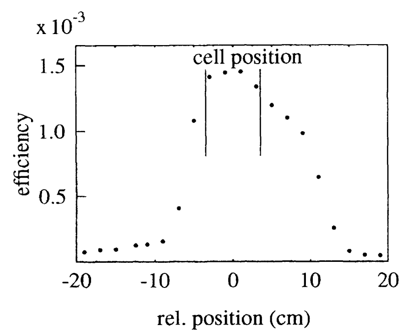

FIG. 6. Total efficiency of the 85% HPGe detector, measured by moving a pointlike calibration source along the beam axis through the scattering chamber. The position of the chamber is shown by the two vertical lines.

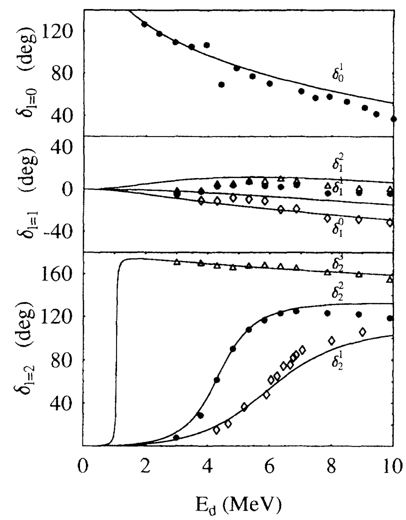

FIG. 7. Phase shifts for s, p, and d waves deduced from experimental ^2H-^4He scattering data given by Refs. [20,28,29]. The solid lines are the result of the present OM calculation.

vector and tensor analyzing powers of $^4He(\vec{d},d)^4He$ scattering in a large range of energies (see [20] and references therein). The results of these analyses for projectile energies between 3 and 10 MeV are presented in Fig. 7.

We have calculated these phase shifts in the framework of the optical model. Neglecting the imaginary part of the potential, since the imaginary phase shifts are small in this energy region [20], the optical potential is given by

$$V(R) = \lambda V_F(R) + \lambda_{s.o.}\frac{1}{R}\frac{dV_F(R)}{dR}\mathbf{L}\cdot\mathbf{s} + V_C(R). \quad (3.1)$$

The first term, the real central potential, is calculated by a double-folding procedure [21,22]:

$$\begin{aligned} V_F(R) = & \int\int \rho_a(\mathbf{r_1})\rho_A(\mathbf{r_2}) \\ & \times v_{\rm eff}(E,\rho_a,\rho_A,s \\ & = |\mathbf{R}+\mathbf{r}_2-\mathbf{r}_1|)d\mathbf{r}_1 d\mathbf{r}_2. \end{aligned} \quad (3.2)$$

The α density is derived from the charge density distribution [23], the deuteron density is calculated in a Reid soft-core potential [24,25]. The effective nucleon-nucleon interaction is assumed to be energy and density dependent [21,22]. The second term in Eq. (3.1), the spin-orbit part, is taken in the usual Thomas form which is proportional to $\frac{1}{R}\frac{dV_F(R)}{dR}$. The Coulomb potential of a homogeneously charged sphere is given by $V_C(R)$.

The strength of both potentials, the real central and the spin-orbit term, is normalized by factors λ and $\lambda_{s.o.}$, respectively, which are fixed to elastic phase shift data. The resulting values for λ are given in Table I. We find

TABLE I. Potential normalization parameters λ and $\lambda_{s.o.}$.

$(-1)^L$	λ	$J_R/(A_P * A_T)$ (MeV fm^3)	r_{rms} (fm)	$\lambda_{s.o.}$ (fm^2)
+1	1.98	675.3	3.183	−0.318
−1	1.80	614.3	3.183	−0.318

TABLE II. Calculated and experimental level scheme of ^{6}Li.

L	S	J^π	E_{exp} (keV)	Γ_{exp} (keV)	E_{calc} (keV)	Γ_{calc} (keV)
0	1	1^+	0	–	−278	–
2	1	3^+	2186± 2	24 ± 2	2186	25
2	1	2^+	4312± 22	1700±100	4275	≈ 2000
2	1	1^+	5650± 50	1500±200	5500	≈ 2000

that the d-α potential is strongly parity dependent. Good agreement between the experimental phase shift data and the phase shifts calculated with our optical model (OM) is obtained (see Fig. 7).

Using this potential we are able to calculate the energy dependence of the ratio of the differential cross sections at the center-of-mass angles $\vartheta_{c.m.} = 96.9^o$ and $\vartheta_{c.m.} = 124°$ which correspond to the scattered α particles and the recoiled deuterons in our particle detector (see Sec. II). Excellent agreement is found between the calculated and measured ratio (see Fig. 5). As mentioned above, this procedure was used to determine the energy of the α particles in the center of the gas cell and to find the 3^+ resonance.

The same potential is used to calculate the relative wave function $u_{NLJ}(R)$ in a cluster model of ^{6}Li= $\alpha \otimes d$ where the oscillator quantum number Q, the node number N, and the orbital angular momentum number L are related to the corresponding quantum numbers of the two nucleons in the deuteron:

$$Q = 2N + L = \sum_{i=1}^{2}(2n_i + l_i) = 2. \tag{3.3}$$

Thus, we obtain the ^{6}Li singlet ground state with $N = 1, L = 0, J^\pi = 1^+$, and the excited triplet states with $N = 0, L = 2 : J^\pi = 3^+, 2^+, 1^+$ (see Table II). The description of the level scheme of ^{6}Li is quite satisfying: the energy of the triplet states 3^+, 2^+, and 1^+ and the width of the 3^+ state are correctly reproduced, while the widths of the 2^+ and 1^+ states are somewhat overestimated. The calculated energy of the ground state is about 1750 keV below the α-d threshold while the experimental binding energy of ^{6}Li is 1475 keV.

IV. CAPTURE CROSS SECTIONS AND DIRECT-CAPTURE MODEL

In the direct-capture (DC) model the capture cross section is given by

$$\sigma_{DC} = C^2 S \cdot \int d\Omega \cdot 2 \left(\frac{e^2}{\hbar c}\right) \left(\frac{\mu c^2}{\hbar c}\right) \left(\frac{k_\gamma}{k_a}\right)^3 \frac{1}{2I_A + 1} \frac{1}{2S_a + 1} \sum_{M_A M_a M_B, \sigma} |T_{M_A M_a M_B, \sigma}|^2. \tag{4.1}$$

The quantities I_A, I_B, and $S_a (M_A, M_B$, and $M_a)$ are the spins (magnetic quantum numbers) of the target nucleus A, residual nucleus B, and projectile a, respectively. The reduced mass in the entrance channel is given by μ. The polarization σ of the electromagnetic radiation can be ± 1. The wave number in the entrance channel and for the emitted radiation is given by k_a and k_γ. The factor C is the isospin Clebsch-Gordan coefficient which couples the isospin of the α particle and the deuteron to the isospin of the residual nucleus ^{6}Li: $C = (0000|00) = 1$, and S is the spectroscopic factor which specifies the probability to find the ^{6}Li nucleus in an α-d cluster configuration: $S = 0.85$ [14].

In our case the transition matrix $T_{M_A M_a M_B, \sigma}$ is dominated by electric quadrupole radiation. Electric dipole transitions are strongly suppressed because the charge-to-mass ratio of projectile and target is nearly identical. Noticeable contributions of $E1$ radiation are expected only below about $E_{c.m.} \approx 150$ keV [12].

The exact formalism was developed by Kim, Park, and Kim [26], and it can be found in [27]. The electromagnetic transition amplitudes T in Eq. (4.1) depend on the overlap integrals of the bound-state wave function u_{NLJ}, the scattering wave function $\chi_{l_a j_a}$, and the electric quadrupole operator $\mathcal{O}^{E2}$:

$$I^{E2}_{l_a j_a} = \int dr\, u_{NLJ}(r)\, \mathcal{O}^{E2}(r)\, \chi_{l_a j_a}(r). \tag{4.2}$$

Both wave functions can be calculated using the same potential parameters which have already been fixed to elastic phase shift data (see Sec. III). That means that no free parameters are needed for the calculation of the capture cross section.

V. RESULTS AND DISCUSSION

In Fig. 8 the experimental results of our investigation are shown together with the results of our calculation in the DC model in the range of the 3^+ resonance. The error bars show statistical errors only.

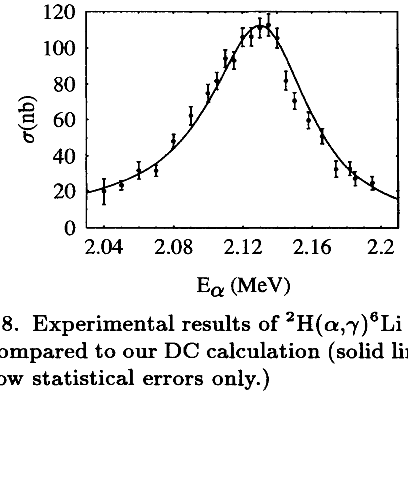

FIG. 8. Experimental results of $^2H(\alpha,\gamma)^6Li$ in the 3^+ resonance compared to our DC calculation (solid line). (The error bars show statistical errors only.)

The absolute values of the cross sections have been determined using the measured efficiency under consideration of the angular distribution of the $E2$ transition. The uncertainty in the absolute value can be estimated to be 10% for one standard deviation. The main contribution is due to the uncertainty of the effective target thickness of the extended gas target ($\approx 10\%$). The uncertainties of solid angle of the particle detector at $\vartheta_{\text{lab}} = 28°$ ($< 5\%$), efficiency of the HPGe detector ($< 5\%$), and neglect of deadtime correction ($< 0.1\%$) are small compared to the main uncertainty.

From the experimental data a total width of the resonance of $\Gamma = (25 \pm 3)$ keV can be extracted which compares well with the adopted value [14] of $\Gamma = (24 \pm 2)$ keV. Assuming a Breit-Wigner shape of the resonance a radiative width $\Gamma_\gamma = (0.43 \pm 0.05)$ meV is obtained which agrees with the value $\Gamma_\gamma = (0.440 \pm 0.034)$ meV taken from an (e, e') experiment [15]. Good agreement is found between the experimental data and the calculated values for both the strength and the width of the resonance.

In Fig. 9 we show our calculated capture cross section for the energy region $E_{\text{c.m.}} \leq 4$ MeV together with the experimental data from Refs. [15,3,5]. The marked region characterizes the range of our experiment which is shown in Fig. 8. For energies lower than 1 MeV, the capture cross section is dominated by the 3^+ resonance at $E_{\text{c.m.}} = 711$ keV.

Our calculation consistently describes the resonant and nonresonant behavior of the capture cross section from about 100 keV up to several MeV. The results of our calculation agree well with those presented by Robertson *et al.* [3] and by Burkova *et al.* [11]. The calculated cross section describes very well the experimental data up to about 3 MeV. But some discrepancies are found between the experimental data and our calculation on the one hand and the calculated results of Typel *et al.* [12] on the other hand. The multichannel resonating group calculation underestimates the capture cross section at low energies strongly and results in a smaller width of the 3^+ resonance.

The new results confirm the predictions of Robertson *et al.* [3] with regard to the synthesis of ^{6}Li in the big bang nucleosynthesis. The reaction rate is too low to lead to a significant amount of ^{6}Li during the big bang compared to the observed abundance of ^{6}Li and the ^{6}Li/^{7}Li ratio. Hence we confirm the assumption that ^{6}Li is mainly produced via spallation processes induced by galactic cosmic rays.

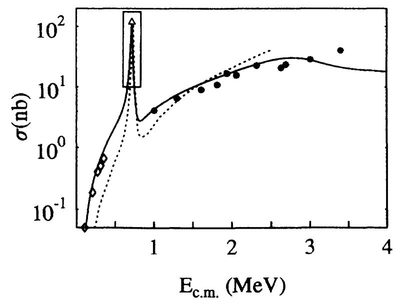

FIG. 9. Experimental results of ^{2}H$(\alpha,\gamma)^6$Li below [5], at [15], and above [3] the 3^+ resonance compared to our DC calculation (solid line) and to the microscopic calculation by Typel *et al.* [12] (dashed line).

VI. SUMMARY

The cross section for the capture reaction ^{2}H$(\alpha, \gamma)^6$Li has been measured in the energy region of the 3^+ resonance in ^{6}Li. The adopted values of the total width Γ and the radiative width Γ_γ for this resonance which stem from different experiments could be confirmed in one direct measurement of the γ quanta of the reaction ^{2}H$(\alpha, \gamma)^6$Li. The energy dependence of the capture cross section can be understood in terms of a direct-capture model using folding potentials for the 3^+ resonance as well as in the nonresonant regions at lower and higher energies.

ACKNOWLEDGMENTS

We would like to thank the accelerator crew and the other members of the Institut für Strahlenphysik der Universität Stuttgart for the kind support of this experiment, and the Deutsche Forschungsgemeinschaft (DFG-projects Sta290/2-2, Sta290/3-1, and Graduiertenkolleg Mu705/3-1) and the Fonds zur Förderung der wissenschaftlichen Forschung in Österreich (project P 8806–PHY).

[1] D. N. Schramm and R. V. Wagoner, Annu. Rev. Nucl. Sci. **27**, 37 (1977).
[2] S. M. Austin, Prog. Part. Nucl. Phys. **7**, 1 (1981).
[3] R. G. H. Robertson, P. Dyer, R. A. Warner, R. C. Melin, T. J. Bowles, A. B. McDonald, G. C. Ball, W. G. Davies, and E. D. Earle, Phys. Rev. Lett. **47**, 1867 (1981).
[4] J. Hesselbarth, S. Khan, Th. Kihm, and K. T. Knöpfle, Z. Phys. A **331**, 365 (1988).
[5] J. Kiener, H. J. Gils, H. Rebel, S. Zagromski, G. Gsottschneider, N. Heide, H. Jelitto, J. Wentz, and G. Baur, Phys. Rev. C **44**, 2195 (1991).
[6] R. Shyam, G. Baur, and P. Banerjee, Phys. Rev. C **44**, 915 (1991).
[7] K. Langanke, Nucl. Phys. **A457**, 351 (1986).
[8] K. Langanke and C. Rolfs, Z. Phys. A **325**, 193 (1986).
[9] R. Crespo, A. M. Eiro, and F. D. Santos, Phys. Rev. C **39**, 305 (1989).
[10] R. Crespo, A. M. Eiro, and J. A. Tostevin, Phys. Rev. C **42**, 1646 (1990).
[11] N. A. Burkova, K. A. Zhaksibekova, M. A. Zhusupov, and R. A. Eramzykan, Phys. Lett. B **248**, 15 (1990).
[12] S. Typel, G. Blüge, and K. Langanke, Z. Phys. A **339**, 335 (1991).
[13] S. Jang, Phys. Rev. C **47**, 286 (1993).
[14] F. Ajzenberg-Selove, Nucl. Phys. **A490**, 1 (1988).
[15] F. Eigenbrod, Z. Phys. **228**, 337 (1969).

[16] J. Kiener, G. Gsottschneider, H. J. Gils, H. Rebel, V. Corcalciuc, S. K. Basu, G. Baur, and J. Raynal, Z. Phys. A **339**, 489 (1991).
[17] U. Hoyler and H. Wäffler, Z. Naturforsch. **26a**, 592 (1971).
[18] A. Galonsky, R. A. Douglas, W. Haeberli, M. T. McEllistrem, and H. T. Richards, Phys. Rev. **98**, 586 (1955).
[19] H. Meiner, E. Baumgartner, S. E. Darden, P. Huber, and G. R. Plattner, Helv. Phys. Acta **40**, 483 (1967).
[20] E. Jenny, W. Grüebler, V. König, P. A. Schmelzbach, and C. Schweizer, Nucl. Phys. **A397**, 61 (1983).
[21] A. M. Kobos, B. A. Brown, R. Lindsay, and R. Satchler, Nucl. Phys. **A425**, 205 (1984).
[22] H. Abele and G. Staudt, Phys. Rev. C **47**, 742 (1993).
[23] H. de Vries, C. W. Jager, and C. de Vries, At. Data Nucl. Data Tables **36**, 495 (1987).
[24] R. Frick, Ph.D. thesis, LMU München, 1980 (unpublished).
[25] R. V. Reid, Jr., Ann. Phys. **50**, 411 (1968).
[26] K. H. Kim, M. H. Park, and B. T. Kim, Phys. Rev. C **35**, 363 (1987).
[27] P. Mohr, H. Abele, R. Zwiebel, G. Staudt, H. Krauss, H. Oberhummer, A. Denker, J. W. Hammer, and G. Wolf, Phys. Rev. C **48**, 1420 (1993).
[28] W. Grüebler, P. A. Schmelzbach, V. König, R. Risler, and E. Boerma, Nucl. Phys. **A242**, 265 (1975).
[29] L. C. McIntyre and W. Haeberli, Nucl. Phys. **A91**, 382 (1967).